International Journal of Nanomedicine

Dovepress
open access to scientific and medical research

Open Access Full Text Article

ORIGINAL RESEARCH

# Response Surface Methodology for Statistical Optimization of Chitosan/Alginate Nanoparticles as a Vehicle for Recombinant Human Bone Morphogenetic Protein-2 Delivery

This article was published in the following Dove Press journal:
*International Journal of Nanomedicine*

Maryam Zohri[1]
Hamid Akbari Javar[2]
Taraneh Gazori[3]
Mohammad Reza Khoshayand[4]
Seyed Hamid Aghaee-Bakhtiari[5,6]
Mohammad Hossein Ghahremani[1,7]

[1]Nanotechnology Research Center, Faculty of Pharmacy, Tehran University of Medical Sciences, Tehran, Iran; [2]Departments of Pharmaceutics, Faculty of Pharmacy, Tehran University of Medical Sciences, Tehran, Iran; [3]Research and Development Department, Trita Nano Pharmaceutical Research Center, Tehran, Iran; [4]Department of Drug and Food Control, Faculty of Pharmacy, Tehran University of Medical Sciences, Tehran, Iran; [5]Bioinformatics Research Group, Mashhad University of Medical Sciences, Mashhad, Iran; [6]Department of Medical Biotechnology, Faculty of Medicine, Mashhad University of Medical Sciences, Mashhad, Iran; [7]Department of Pharmacology and Toxicology, Faculty of Pharmacy, Tehran University of Medical Sciences, Tehran, Iran

**Purpose:** In this study, chitosan/alginate nanoparticles are prospected as a carrier for controlled release of recombinant human bone morphogenetic protein-2 (rhBMP-2).

**Materials and Methods:** The rhBMP-2-loaded chitosan/alginate nanoparticles (Cs/Alg/B NPs) were prepared using the ionic gelation (IG) method. The current research was conducted to optimize the effective factors for entrapping rhBMP-2 in Cs/Alg NPs using response surface methodology (RSM) and the Box–Behnken design (BBD). The variables were the Cs/Alg molecular weight (Mw) ratios (1–3), pH (4.8–5.5), stirring rates (900–1300 rpm) and the responses included size, ζ-potential, polydispersity index (PDI), loading efficacy (LE), cumulative release (CR), and morphological degradation time (MDE). Then, the morphological properties of optimum formulation were studied for post-characterization. In the next step, the MTT assay for the optimized run was done for 24 and 48 hours.

**Results:** The results revealed that the optimum conditions for the mentioned variables were stirring rate=1100 rpm, pH=5.15, and Cs/Alg Mw ratio=1.75 based on numerical optimization. It was shown that the average particle size and loading efficacy at optimum conditions were 253 nm and 67%, respectively. Other responses were as follows: CR=66%, ζ-potential= +35mV, PDI=0.5, and MDT=7 days.

**Conclusion:** The results have suggested that the statistical optimization of rhBMP-2 offers the possibility of preparing Cs/Alg/B NPs with a favorable size, controlled release characteristics, and high loading efficiency. It is expected that the acquired optimum conditions will be useful for efficient rhBMP-2 delivery.

**Keywords:** alginate, Box–Behnken design(BBD), chitosan, response surface methodology (RSM), recombinant human bone morphogenetic protein-2 (rhBMP-2), chitosan/alginate nanoparticles

## Introduction

Growth factors are natural molecules with a protein or steroid structure involved in the growth and differentiation of many cells.[1] Bone morphogenetic proteins (BMPs) belong to the transforming growth factor-β (TGF-β) superfamily. They are composed of amino acid sequences with more than 35 members and classified into several subgroups including; BMP (−2 and −4), BMP (−5, −6, −7, and −8) and BMP (−9, −10, and −15).[2,3] BMP-2 is composed of 114 amino acids and has an Mw of about 32 KDa. It regulates the differentiation of mesenchymal stem cells (MSCs) through the

Correspondence: Mohammad Hossein Ghahremani
Tel/Fax +9866959102
Email mhghahremani@tums.ac.ir

submit your manuscript | www.dovepress.com
DovePress
http://doi.org/10.2147/IJN.S250630

Smad pathway.[4] It can be either isolated from a native bone or expressed as a recombinant human bone morphogenetic protein-2 (rhBMP-2).[5] Recent therapies based on using growth factors delivery have increased in the field of tissue engineering. However, despite the progress in this area, the success rate of clinical trials using rhBMP-2 is not noticeable due to some limitations like the high cost of production, large molecular size, the need for physiological doses, failure to maintain the long-term concentrations, and toxic potency at high doses.[6] Encapsulation is a technology for placing various substances including liquids, solids, and gases into a homogeneous or heterogeneous coating in a continuous underlying material to protect, stabilize, and controlled release of the encapsulated compounds.[7] Among a variety of natural components like alginate, albumin, or chitosan that have been extensively investigated, polymeric NPs have demonstrated the ability to deliver growth factors.[8] Chitosan is a glucan derivative with repeated units of chitin composed of D-glucosamine and N-acetyl-D-glucosamine. It is also cationic, biodegradable and has free amino groups with positive charges that give it the possibility to react with the cell membrane, alginate, and other anionic polymers.[9] Alginate, as a component of the cell wall of brown algae, is sodium alginic acid with linear chains of α-L-glucuronic acid (G) and β-D-mannuronic acid (M). The main advantages of using chitosan and alginate over the other materials for nanoparticles (NPs) preparation include their good biocompatibility, biodegradability,[4] and non-toxic properties.[10,11] There are several methods for the preparation of polymeric NPs like solvent evaporation, nanoprecipitation, salting-out, dialysis, supercritical fluid technology, and ionotropic gelation.[12] Ionotropic gelation (IG) is the ability to form a hydrogel through crosslinking of cationic and negatively charged ingredients by the counter ions.[13] This method is regularly used for the preparation of polymeric NPs due to the advantages like NPs formation in very mild conditions (averting high shear forces) and avoiding harmful organic solvents. Other advantages of this method include the protection of protein structure which leads to keeping its functionality. According to this method, Cs/Alg NPs can be produced in a two-step procedure by polycationic crosslinking in the presence of a polyanion like calcium chloride.[14] Studies using chitosan NPs for rhBMP-2 sustained release in Sprague-Dawley rats indicates a promising carrier for rhBMP-2 delivery.[15] Another study incorporated rhBMP-2 to chitosan-based microspheres for the accelerated repair of rabbit mandibular defects.[16] Response surface methodology (RSM) use for the development and optimization of drug carriers extensively. It is a set of statistical techniques use for the optimization of operational factors with minimal confounding.[17] Accordingly, the number of experiments is reduced and all coefficients of the second-order regression model and the effects of factors are calculated. Depending on their application in design expert, RSM can be performed by different methods like Central Composite Design (CCD), D-Optimal, and Box–Behnken design (BBD).[18] The Box–Behnken is an incomplete three-level factor design. In this method, a two-level test block method is repeated between different sets of variables.[19] In one study, RSM was also used to investigate the optimized condition for rhBMP-2 encapsulation (including high LE, PDI, and high local sustained delivery) and to improve the encapsulation of rhBMP-2 using polyvinyl alcohol carriers, which resulted in the highest encapsulation efficiency (76.5%).[20] In another research also statistical optimization of chitosan NPs as protein vehicle, using RSM, was evaluated and found to be promising for protein entrapment into tripolyphosphate (TPP) cross-linked chitosan NPS.[21] In the current study, Cs/Alg NPs was employed as a carrier for rhBMP-2, and RSM was used to optimize parameters of the preparation. Concerning the importance of growth factors, optimization for finding the best formulation can be helpful for delivery of NPs to the appropriate targets with the right dosage, and minimal side-effects. We have studied the details for optimized rhBMP-2-loaded Cs/Alg NPs prepared with the ionotropic gelation method and considering the optimal conditions of variables (Cs/Alg $M_w$ ratios, pH, stirring rates). The responses including the size, LE, ζ-potential, PDI, CR, and MDT were optimized.

# Materials and Methods

## Materials

Sodium alginate (20–40 kDa), low Mw chitosan (90% deacetylation, 50–190 kDa, based on viscosity), recombinant human bone morphogenetic protein-2 (rh BMP-2, 26 kDa), Spectra/Por Float-A-Lyzer G2 dialysis (MW cut-off 50 kDa) and MTT (3-(4, 5-Dimethylthiazol-2-yl)-2, 5-diphenyltetrazolium bromide) were purchased from Sigma-Aldrich (St. Louis, MO, USA). Amicon® Ultra-15 centrifugal filter unit 50 kDa, calcium chloride, and dimethyl sulfoxide (DMSO) were obtained from Merck Millipore (Germany). RPMI 1640 medium, penicillin-streptomycin solution 100X, and fetal bovine serum (FBS) were provided from Biowest (Riverside, MO, USA).

# Methods

## Experimental Design

RSM was applied for optimizing the preparation conditions of Cs/Alg/B NPs using Design-Expert® software (Trial version 12; Stat-Ease Inc., Minneapolis, MN, USA). In this method, the correlations between the responses and factors were also investigated. The Box–Behnken design (BBD) was applied for optimization. Three independent variables (pH, stirring rate, and Cs/Alg molecular weight ratio (Mw)) were studied for their effects on responses (dependent factors) including $Y_1$=particle size, $Y_2$=LE, $Y_3$=CR, $Y_4$=ζ-potential, $Y_5$=PDI, and $Y_6$=MDT. As shown in Table 1, the concentration ranges using (−1, 0, 1), indicating low, medium, and high, respectively, were selected based on preliminary experiments in developing NPs and similar published data on rhBMP-2-loaded NPs.[20]

## Nanoparticle Preparation

Cs/Alg/B NPs were synthesized using the ionotropic gelation method. For the synthesis procedure, the stock solutions of chitosan (10 mg/mL) in 1% (v/v) acetic acid, sodium alginate (10 mg/mL), and calcium chloride (10 mg/mL) were prepared in deionized water. Before using the stocks, a syringe filter (0.22 µm) was used for filtration. Particles were prepared under sterile conditions. First, 130 µL of the sodium alginate stock solution (10 mg/mL) was diluted with up to 3 mL of filtered deionized water as a working solution. Then, 26 µL of calcium chloride solution (10 mg/mL) was diluted up to 1 mL of filtered deionized water as the working solution and added dropwise to the alginate solution with a final volume of 4 mL under magnetic stirring condition (in the pre-gelation stage in various stirring rates, as seen in Table 1) for 15 minutes. The final pH and Cs/Alg Mw ratios were adjusted according to Table 1. Then, 4 µL of rhBMP-2 (1 µg/100 µL) was added and stirred at the specified speed for each run (Table 1) for 30 minutes. Next, 25 µL of chitosan stock with Cs/Alg Mw ratios of 0.5, 1.75, and 3 (Table 1) were diluted up to 1 mL with deionized water. Chitosan was then used for formation of Cs/Alg/B NPs added dropwise to present the solution for a further 45 minutes under stirring conditions (Table 1). After the formation of Cs/Alg/B NPs were separated from free polymers and free rhBMP-2 by centrifugation at 3214 g for 20 minutes by using an Amicon® Ultra-15 centrifugal filter unit at 50 kDa.[10,21]

## Cs/Alg/B NPs Characterization

### Size, ζ-Potential, and Polydispersity Index (PDI)

Size, ζ-potential, and PDI of all runs were measured in triplicate by using Zetasizer 3000 HS (Malvern Instruments, UK).[24]

### In vitro Analysis of Loading Efficacy (LE)

LE of rhBMP-2 was measured for all runs as follows: firstly formulations were ultracentrifuged at 3214 g for up to 20 minutes at 25°C using Amicon Ultra-15 (Ultracel-50K Millipore Co., USA) Mw cut-off of 50 kDa to remove naked rhBMP-2 and free polymer molecules. In the next step, the supernatant collected in the inner layer of ultrafilter, diluted with phosphate (1:1 v/v) buffer, and resulting solution absorbance were measured at 450 nm using a UV/VIS spectrophotometer (Shimadzu UV-1800).[22] The empty (placebo) Cs/Alg NPs were used as blank. LE was calculated using equation (1):

$$\text{Loading efficacy(LE\%)} = \frac{(\text{Wt} - \text{Wf})}{\text{Wt}} \times 100 \quad (1)$$

where Wt=Weight of total rh BMP-2 used in Cs/Alg/B NPs(ng) and Wf=Weight of free rh BMP-2 (ng).

### In vitro Analysis of Cumulative Release (CR)

To calculate the cumulative release percentages of the rhBMP-2 in each run, 0.5 g of rhBMP-2-loaded NPs were incubated in 2 mL phosphate buffer solution (PBS, pH=7.4) within a Float-A-Lyzer G2 Dialysis Device MWCO 50KD (Spectra-Por, Sigma Aldrich), at 37°C by applying gentle shaking (50 rpm) for 0, 3, 7, 10, 12, 14, and 28 days. Media aliquots were collected regularly and substituted with fresh PBS. Then the amount of rhBMP-2 was analyzed by an ELISA kit (R&D Systems, Inc., Minneapolis, MN, USA). The absorbance was measured at 450 nm, and CR (%) was calculated for every run during the mentioned days in the indicated time points. Then total release for every run was reported as a cumulative release percentage.[23]

# Nanoparticle Morphological Change Measurement (Morphological Degradation Time)

Morphological changes of Cs/Alg/B NPs were observed using SEM (Flex SEM 1000, Hitachi, Japan). Morphological changes are shown in Figure 1, and the average time for degradation of each run until the appearance of degradation shape was evaluated.[25]

**Table 1** The Data from Experimental Design of Independent Variables for Optimization of Cs/Alg/B NPs

| Variables and Their Levels in the Experiment Design | | | | | | | |
|---|---|---|---|---|---|---|---|
| **Independent Variables** | **Symbol** | **Levels** | | | **Dependent Variables** | **Units** | **Constraints** |
| | | **−1** | **0** | **1** | | | |
| pH | A | 4.8 | 5.15 | 5.5 | Y1=Particle Size (PS) | nm | Minimize |
| | | | | | Y2=Loading efficacy | % | Maximize |
| Cs/Alg Mw ratio | B | 0.5 | 1. 75 | 3 | Y3=Polydispersity index (PDI) | - | Less than 0.5 |
| | | | | | Y4=ζ-potential | mv | Maximize |
| Stirring rate (rpm) | C | 900 | 1100 | 1300 | Y5=Cumulative Release (CR) | % | Maximize |
| | | | | | Y6=Morphological degradation time (MDT) | Day | Maximize |

| Experimental design matrix and results of Box–Behnken design | | | | | | | | | |
|---|---|---|---|---|---|---|---|---|---|
| | **Independent variables** | | | **Dependent variables** | | | | | |
| **Run** | **A** | **B** | **C** | **Size (nm)** | **LE (%)** | **CR (%)** | **ζ-potential (mV)** | **PDI** | **MDT** |
| 1 | 0 | 0 | 0 | 525 | 25 | 15 | 34.3 | 0.62 | 4 |
| 2 | 1 | 0 | 1 | 611 | 19 | 10 | 34 | 0.7 | 4 |
| 3 | 0 | 0 | 0 | 522 | 27 | 17 | 35 | 0.65 | 4 |
| 4 | 1 | 1 | 0 | 898 | 22 | 12 | 23 | 0.8 | 2 |
| 5 | 0 | −1 | −1 | 189 | 76 | 66 | 22 | 0.4 | 14 |
| 6 | 0 | −1 | 1 | 256 | 70 | 60 | 23 | 0.55 | 12 |
| 7 | −1 | 0 | 1 | 557 | 22 | 15 | 38 | 0.7 | 3 |
| 8 | 0 | 1 | −1 | 802 | 20 | 10 | 23 | 0.72 | 2 |
| 9 | 1 | −1 | 0 | 275 | 72 | 60 | 23 | 0.6 | 13 |
| 10 | 0 | 0 | 0 | 523 | 25 | 16 | 37 | 0.67 | 4 |
| 11 | 0 | 1 | 1 | 900 | 19 | 15 | 39 | 0.86 | 3 |
| 12 | −1 | −1 | 0 | 235 | 70 | 61 | 24 | 0.5 | 13 |
| 13 | 0 | 0 | 0 | 520 | 29 | 19 | 37 | 0.61 | 5 |
| 14 | 0 | 0 | 0 | 519 | 27 | 18 | 35 | 0.56 | 4 |
| 15 | −1 | 0 | −1 | 501 | 25 | 18 | 33 | 0.63 | 4 |
| 16 | −1 | 1 | 0 | 811 | 20 | 15 | 23 | 0.76 | 3 |
| 17 | 0 | −1 | −1 | 598 | 17 | 11 | 33 | 0.68 | 4 |

| Analysis of variance for Box–Behnken design refined models | | | | | | | |
|---|---|---|---|---|---|---|---|
| **Dependent Variables** | **Source of Variations** | **Mean Square** | **F-value** | ***P*-value > F** | **$R^2$** | **Adjusted $R^2$** | **Predicted $R^2$** |
| Particle size (PS) | Model Lack of fit | 85155.65 | 534.47 | ‹0.0001 | 0.9985 | 0.9967 | 0.9772 |
| Polydispersity index (PDI) | Model Lack of fit | 0.020 | 8.46 | 0.0051 | 0.9158 | 0.8075 | 0.1676 |
| ζ-potential | Model Lack of fit | 70.90 | 45.96 | ‹0.0001 | 0.9834 | 16.074 | 0.8742 |
| Morphological degradation time (MDT) | Model Lack of fit | 31.53 | 196.77 | ‹0.0001 | 0.9954 | 0.9676 | 0.9896 |
| Cumulative release (CR) | Model Lack of fit | 765.09 | 212.10 | ‹0.0001 | 0.9963 | 0.9624 | 0.9916 |
| Loading efficacy (LE) | Model Lack of fit | 836.91 | 117.28 | ‹0.0001 | 0.9934 | 0.9159 | 0.9849 |

## Optimization and Validation of the Applied Model

To achieve the optimum conditions for dependent variables, 3D surface plots, and contour plots were obtained from the software (Figures 2 and 3 and Supplementary Figures 1–4). The optimized point and solutions for constraints were calculated using numerical optimization. The optimum values, for responses, the minimum particle size, maximum LE, CR, MDT, ζ-potential, and, PDI less of 0.5 were selected. Accordingly, to find and evaluate the responses, the optimal condition for the production of Cs/Alg/B NPs was found according to the constraints. The model predicted a particle size of 253 nm, LE of 67%, CR of 66%, a ζ-potential of 35 mV, PDI of 0.5, and MDT of 7 days. The predicted point condition followed: stirring rate=1100, pH=5.15, and Cs/Alg Mw ratio=1.75. The model was validated and examined by running

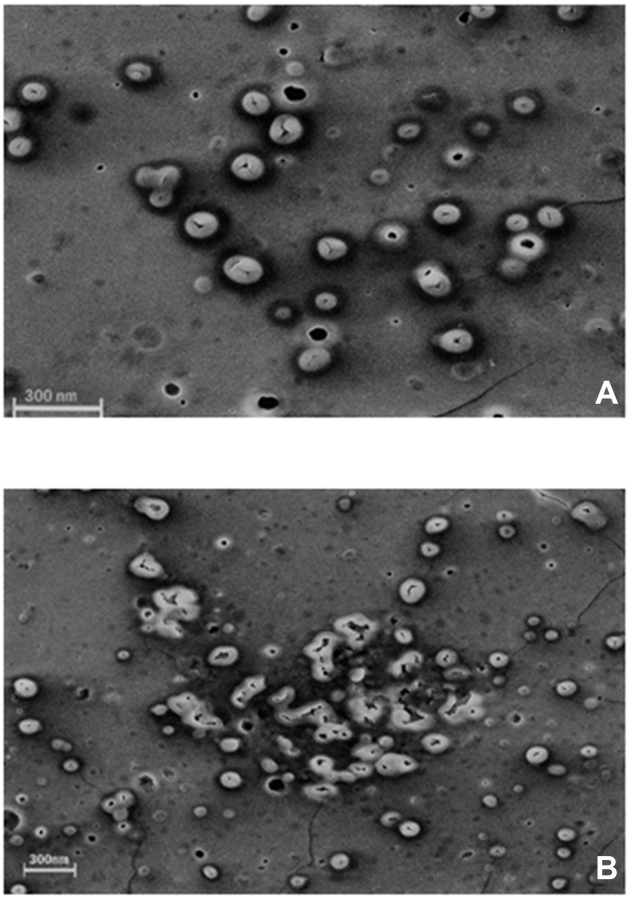


**Figure 1** SEM images of morphological degradation of Cs/Alg/B NPs. (**A**) The initial stage of degradation on the 7th day of preparation. (**B**) End-stage of morphological degradation after the 14th day of preparation. For each run MDT is included in optimization as a quantitative factor. The scale bar is 300 nm. More images are shown in Supplementary Figure 5.

five experiments using the optimum conditions, as mentioned previously. The perfect agreement between the observed values and predicted point by DOE certified the statistical significance of the model as well as their adequate precision for the prediction of the optimum condition in the domain of levels chosen for independent variables.

## Post Characterization Evaluation of the Optimized Cs/Alg/B Nanoparticles

### Morphology of Optimized Cs/Alg/B NPs

Morphological analysis of the optimized Cs/Alg/B NPs was performed using an SEM (Flex SEM 1000, Hitachi, Japan). After the coating Cs/Alg/B NPs via gold under vacuum,the average size of Cs/Alg/B NPs was measured using the Image J software 1.52 n.[24]

### In vitro Cytotoxicity Study of the Optimized Formula

The NIH 3T3 cell line was obtained from the Pasteur Institute of Iran. The cells were seeded in a 96-well plate at the concentration of $2\times10^4$ cells/well, in triplicate, in the RPMI 1640 medium with 10% FBS and cultured at 37°C in a 5% $CO_2$ condition for 24 and 48 hours. To assess the cytotoxicity of the Cs/Alg/B NPs, the optimized formulation (Cs/Alg Mw ratio=1.75, stirring rate=1100 rpm, pH=5.15) according to the Design Expert results was compared with chitosan (0.25 mg), sodium alginate (1.3 mg), and Cs/Alg/B NPs (40 ng) in terms of the viability of cells at 24 and 48 hours. After exposure, the cells were incubated with MTT=0.5 mg/mL at 37ºC for 4 hours. The medium was removed and the formazan crystals were dissolved in 100 µL DMSO. The absorbance was quantitatively measured at 570 nm using a microplate reader. The results were calculated as the viability percentage and reported as mean±SD.[26] The experimental data were analyzed by two-way analysis of variance (ANOVA) followed by Bonferroni posttest using GraphPad Prism Software Version 8.4.3 (GraphPad Software, San Diego, CA, USA). Differences were considered significant at $P\leq0.05$.

# Results and Discussion

## Nanoparticle Size

Based on experimental design, the Cs/Alg/B size ranged from 189–898 nm (Table 1) which was confirmed by an SEM (Figure 4). This can explain that pH is a crucial factor that influence the size of NPs. This effect can relate to the isoelectric point which there is no net electrical charge on the molecule carriers. It seems that the pH of the chitosan solution with weak polyelectrolyte properties can affect the electric charge density of Cs/Alg/B NPs. The amine groups of the chitosan molecules have a rather low pKa value, at 6.5, and are positively charged at pH values below 6.5.[27] Within runs by increasing pH, the solubility of chitosan was decreased and the pH of Cs/Alg/B NPs solution became close to their isoelectric point, leading to flocculation and sedimentation development and an increase in the size of nanoparticles[28] by reducing the pH to 4.8, the size of the Cs/Alg/B NPs decreased (Figure 2A and D). On the one hand, changing the final pH of the Cs/Alg solution alters the degree of protonation constant (pKa), which reflects the number of binding sites in chitosan molecules (Pka=6.51).[29] To shed more light on the issue, due to the poor solubility of chitosan (which is soluble in acetic acid 1%), the solution likely precipitates upon addition to the alginate solution with pH=5.5. Moreover, between Cs/Alg/B NPs that have less chitosan in formulation (decreasing Cs/Alg Mw ratios), the larger part of amine groups deprotonate (due to pH changes), and the number of functional groups of the chitosan

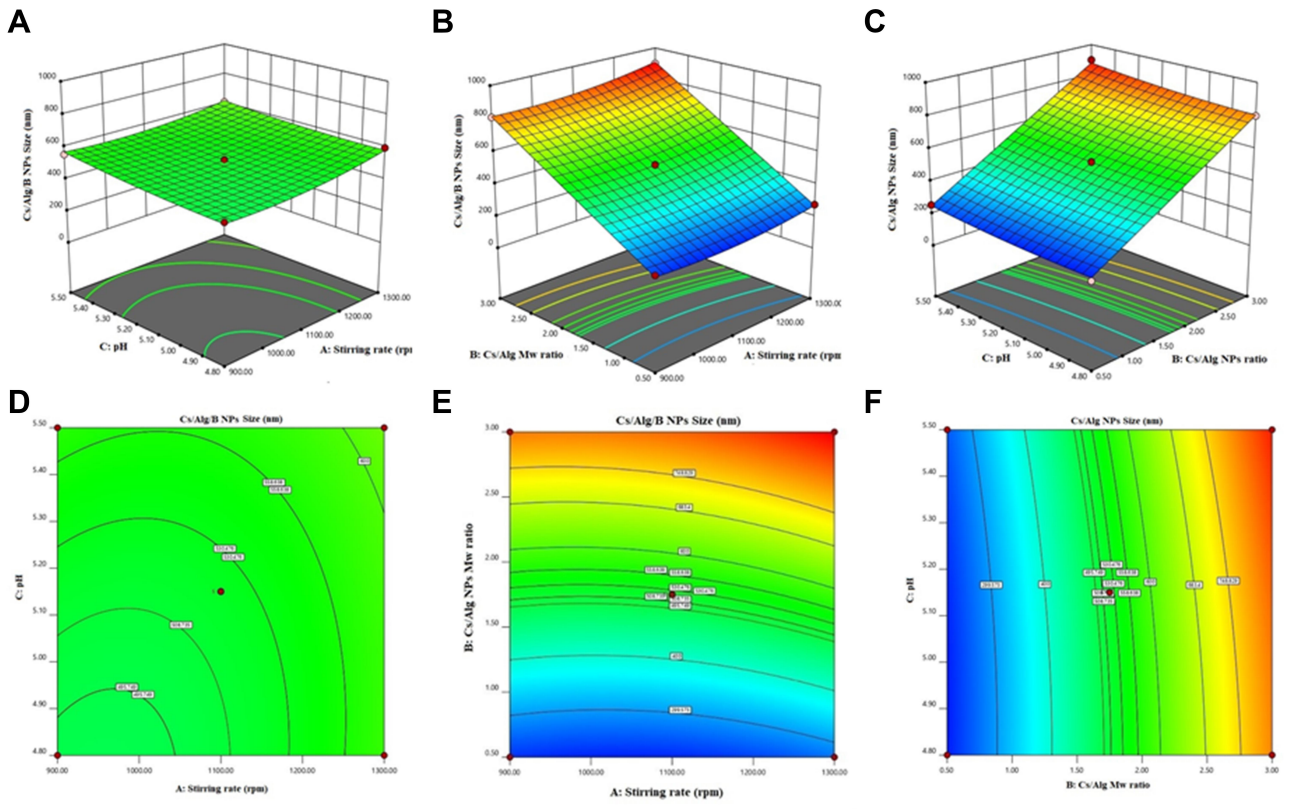


**Figure 2** 3D Response surface plots (**A**–**C**) and contour plots (**D**–**F**) for the mean particle size of Cs/Alg/B NPs. 3D and contour graphs are the preservative relative relationship between two variables on the size of Cs/Alg/B NPs. Contour plots show a three-dimensional surface on a two-dimensional plane. It graphs two predictor variables, X and Y, on the y-axis and a response variable, Z, as contours. Cs/Alg/B NPs, rhBMP-2-loaded chitosan/alginate nanoparticles.

which can participate in particle formation and ionic interactions decrease. Following such events, weaker electrostatic bonds are formed between alginate gel and free polymers in the solution and larger particles appear.[7] Figure 2B and E illustrate the relationship between the Cs/Alg Mw ratios and Cs/Alg/B NPs size. It is shown that the Cs/Alg/B NPs size is significantly ($P \leq 0.05$) increased from 189 to 898 nm when the Cs/Alg Mw ratios increased from 1 to 3. When the Cs/Alg Mw ratios increase from 1 to 3, fewer $H^+$ ions are released from acetic acid ($CH_3COO^-H^+$) that cannot protonate $NH_2$ completely.[30] It is the main reason for reduction of protonation in the unequal Cs/Alg Mw ratios and, therefore, the probability of ionotropic interactions between chitosan and alginate molecules decrease.[31] Also, the alginate solution can share its hydroxide ions. This situation causes unequal interactions in the Cs/Alg/B NPs structure, and free molecules of chitosan accumulate on the surface of NPs which increase the size of Cs/Alg/NPs .[24] An increase in the particle size is also expected due to the presence of intermolecular hydrogen bonding (due to –OH groups of alginate) and intermolecular electrostatic repulsion (due to $-NH_3^+$ of chitosan). Table 1 and Figure 2B and E demonstrate that the stirring rate, especially more than 1000 rpm, was increased with the size of Cs/Alg/B NPs. This result explains that the Cs/Alg NPs receive the energy from stirring in the form of kinetic energy (especially in stirring rates more than 1000 rpm) which can reduce the Mw of chitosan co-polymers. It can also break the initial cross-link between Cs/Alg/B NPs so the initial particles break into smaller fragments and participate or agglomerate and the size of Cs/Alg/B NPs also increase.[32] The relationships between variables for size based on acquired data is shown in equation 2:

$$Y1 = 521.80 + 34.70X + 305Y + 27.25Y + 11.75XY - 10.75XZ + 11.75YZ + 29.47X2 + 3.47Y2 + 15.47Z2 \quad (2)$$

where Y1 is the particle size, X is the stirring rate, and Y and Z are Cs/Alg Mw ratios and pH of the final Cs/Alg/B NPs solution, respectively.

## Loading Efficacy of rhBMP-2

The efficacy of rhBMP-2 loading onto Cs/Alg NPs has been calculated in this study. The results of LE for rhBMP-2 are presented in Table 1. The results showed

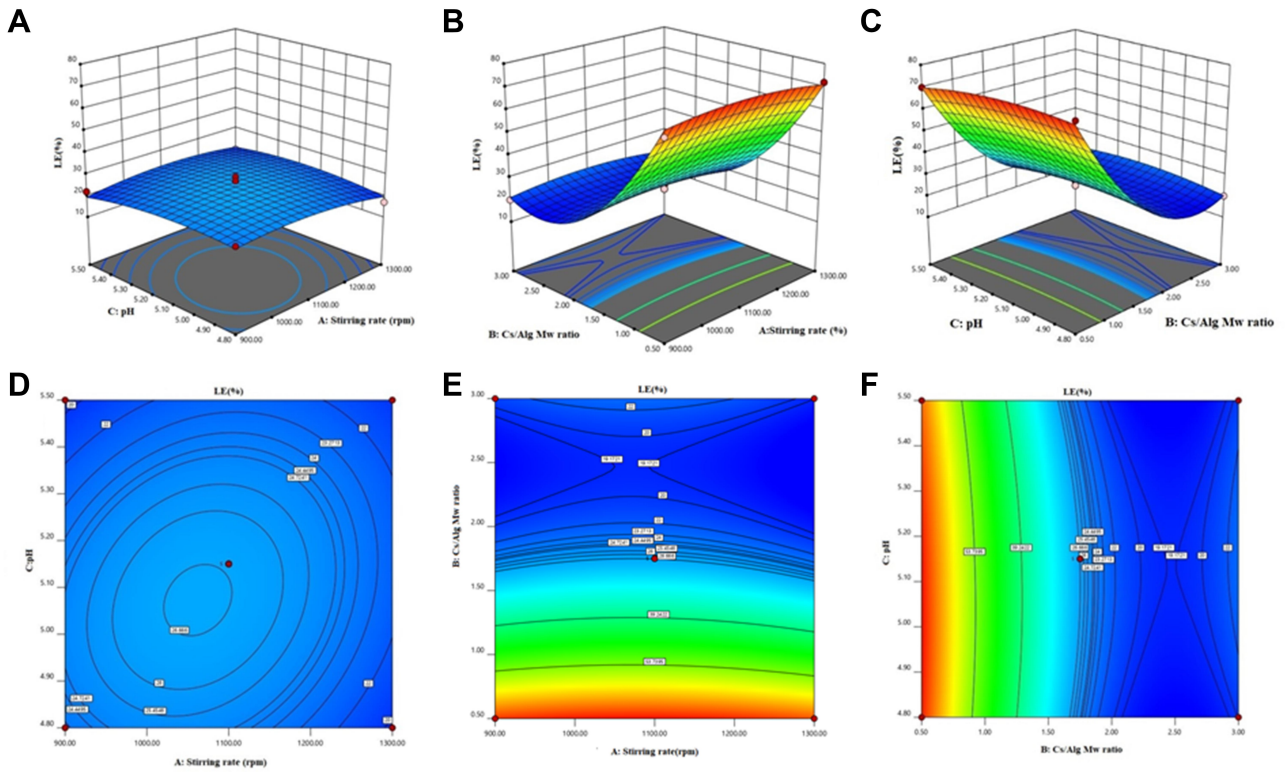


**Figure 3** 3D Response surface plots (**A**–**C**) and contour plots (**D**–**F**) for the mean LE of Cs/Alg/B NPs. 3D and contour graphs are the preservative relative relationship between two variables on the size of Cs/Alg/B NPs LE (%). Contour plots show a three-dimensional surface on a two-dimensional plane. It graphs two predictor variables, X and Y, on the y-axis and a response variable, Z, as contours. LE, loading efficacy (%); Cs/Alg/B NPs, rhBMP-2-loaded chitosan/alginate nanoparticles.

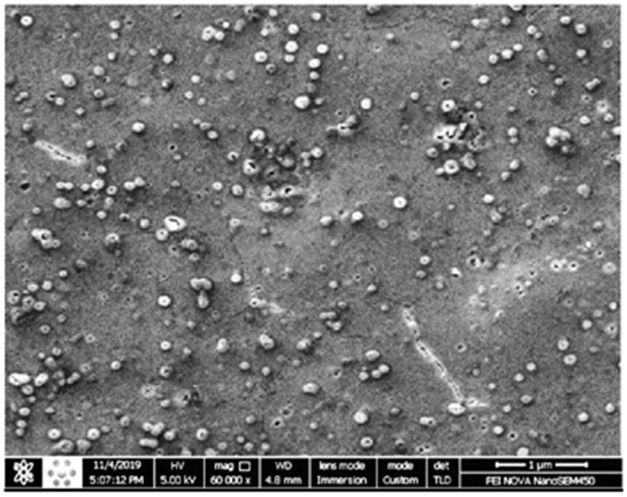

**Figure 4** SEM micrographs of Cs/Alg/B NPs prepared with the optimum formulation of Cs/Alg/B NPs with variables as; Cs/Alg Mw ratio=1, stirring rate=5, pH=5.3 at preparation day. The scale bar is 1 μm.

that the LE of rhBMP-2 reduced when pH increased (Figure 3A and D). Stirring power provides the required energy for the formation of Cs/Alg/B NPs; however, the formed interactions break in the high stirring rates (more than 1100 rpm), which lead to a reduction of LE (Figure 2B and E). One of the effective factors in the LE of NPs is stability. The change in pH values alters the surface charge of the NPs, ζ-potential, and finally their stability. In nanoparticles with ζ-potential values above 30 mV (positive or negative values), the stability increases and the aggregation phenomena slow down due to the repulsion within the particles. A decrease in the ζ-potential due to the electrostatic repulsion is considered as the cause of the aggregation phenomena.[23] The isoelectric point of BMP-2 is equal to 8.2.[33] In higher Cs/Alg Mw ratios, rhBMP-2 cannot interact with chitosan and alginate due to the nanoparticle aggregation and the LE decreases (Figure 3C and F). Generally, in pH values close to the isoelectric point, protein has the minimum surface charge, which induces minimum electrostatic repulsion. Therefore, with an increase in the pH value, the capacity of Cs/Alg NPs for entrapping rhBMP-2 also diminishes. According to the results, with an increase in the final pH of Cs/Alg/B NPs from 4.8 to 5.5, the LE of rhBMP-2 reduced, and the highest LE has been observed at pH values around 4.8 (Table 1). On the other hand, a reduction in the particle size allows more bond formation between Cs/Alg and rhBMP-2, which leads to improved LE. These findings

are consistent with previous studies that reported an increase in the LE when the particle size decreased.[30,34] The relationships between variables for LE based on acquired data is shown in equation 3:

$$Y2 = 26.60 - 0.87X - 25.87Y - Z + 1.25XZ + 1.25YZ - 3.05X^2 + 22.45Y^2 - 2.80Z^2 \quad (3)$$

where Y2 is the LE, X is the stirring rate, and Y and Z are Cs/Alg Mw ratios and pH of the final Cs/Alg/B NPs solution, respectively.

## Cumulative Release of rhBMP-2

According to Table 1, the rhBMP-2 CR (%) has ranged between 10–66% which declined as the size of the Cs/Alg/B NPs increased (Supplementary Figure 1A and D). There are three primary mechanisms for the release of an encapsulate from a carrier; swelling, diffusion, and degradation. One release system may include one or all of them.[35] There is one "Egg-Box" model between chitosan and alginate molecules with the participation of calcium ions.[36] Cs/Alg/B NPs cumulative release can be explained by water absorption and swelling of Cs/Alg/B NPs and the appearance of pores or cracks on their surfaces in the polymer matrix (Figure 4), followed by the burst release of the rhBMP-2 from the "Egg-Box" model of the Cs/Alg NPs. Therefore, small size NPs (in lower pH levels) have a large contact surface that increases the surface porosity as well as the CR (%) (Supplementary Figure 1A and D). In this study, CR (%) of rhBMP-2 increased in formulations with higher LE. On the other hand, the CR (%) decreased with an increase in the Cs/Alg Mw ratios, which can be explained by the fact that in higherCs/Alg Mw ratios, free polymers accumulate around the particles (Supplementary Figure 1B and E). Over time, with an increase in free polymer accumulation, the thickness of the outer layer of the Cs/Alg/B NPs increased, which reduced the possibility of the pore formation on the surface of the Cs/Alg/B NPs as mentioned earlier and decreased the CR(%) of rhBMP-2. Similar results were also observed in the previous studies.[38] Changing the stirring speed was also affected by the release of rhBMP-2 (as shown in Supplementary Figure 1C and F). At higher stirring rates (more than 1100 rpm) CR(%) of rhBMP-2 diminished.[37] The release of the drug and polymer into the media depends on the agitation speed of the systems.[38] A faster and higher drug release has occurred and the mean size of the Cs/Alg/B NPs increased when the rate of stirring has been increased from 900 to 1100 rpm (Table 1). In stirring rates more than 1100 rpm, because of transferring high levels of energy and decreasing the possibility of Cs/Alg/B NPs formation and arrangement, LE has also been decreased and, considering a direct relationship between LE and CR, Cs/Alg/B NPs release also reduced. The relationships between variables for CR based on acquired data is shown in equation 4:

$$Y3 = 17.00 - 2.00X - 24.38Y - 0.62Z - 0.50XY + 0.50XZ + 2.75YZ - 2.13X^2 + 22.13Y^2 - 1.37Z^2 \quad (4)$$

where Y3 is the CR (%), X is the stirring rate, and Y and Z are Cs/Alg Mw ratios and pH of the final Cs/Alg/B NPs solution, respectively.

## ζ-Potential and Polydispersity Index (PDI)

In a colloidal system, stability is a crucial factor that is determined by the magnitude of ζ-potential.[31] In Table 1, the ζ-potential of Cs/Alg/B NPs increased from +22 to +39mV as the Cs/Alg Mw ratios increased. With an increase in the Cs/Alg Mw ratios, more chitosan molecules show a tendency towards each other and form a single larger particle through crosslinking with alginate molecules. Therefore, in low Cs/Alg Mw ratios, when the free H+ ions from the acetic acid are not sufficient to neutralize the hydroxide ions ($OH^-$) of alginate, the $OH^-$ ions tend to ionically cross-link with the protonated $NH_3^+$ groups of chitosan, reducing the ζ-potential of the Cs/Alg/B NPs. In Supplementary Figure 2B and E, pH had a significant effect on the ζ-potential. The ζ-potential is diminished gradually until pH = 4.8 (Supplementary Figure 2A and D). In general, rhBMP-2 contains $NH3^+$ and $NH2^+$ which reacts with $H^+$ ions released from acetic acid and that is fully used up to protonate the $NH_2$ groups on the backbone of chitosan.[40] ζ-potential decreased with an increase in the stirring rate from 900 to1300 rpm due to the instability of the crosslink between chitosan and alginate, as shown in Supplementary Figure 2C and F. In Figure 4A–F, the effect of pH, stirring rate, and Cs/Alg Mw ratios on the formation and stability of Cs/Alg/B NPs was based on their PDI. These results indicate that the formation of stable and homogeneously dispersed Cs/Alg/B NPs significantly depends on the pH value of chitosan and alginate solution used for synthesis. Generally, pH of alginate affects its electronegative potential and its reaction with chitosan. At lower pH values, alginate is buffered by positive ions in the solution ($H_3O^+$ and $H^+$); therefore, it has a lower tendency for

reaction with chitosan. In this condition, Cs/Alg/B NPs with smaller sizes are formed which are more monodisperse.[41] The relationships between variables for ζ-potential (Y4) and PDI (Y5) based on acquired data are shown in equations 5 and 6:

$$Y4 = 35.66 - 0.62X - 0.037Y + 0.89Z + 0.25XY - 1.00XY - 1.02YZ + 0.51X2 - 2.42Y2 - 1.67Z2 \quad (5)$$

where Y4 is the ζ-potential, X is the stirring rate, and Y and Z are Cs/Alg Mw ratios and pH of the final Cs/Alg/B NPs solution, respectively.

$$Y5 = 0.62 + 0.024X + 0.14Y + 0.047Z - 0.015XY - 0.013XZ - 2.500YZ + 0.044X2 - 1.000Y2 + 0.011Z2 \quad (6)$$

where Y5 is the PDI, X is the stirring rate, and Y and Z are Cs/Alg Mw ratios and pH of the final Cs/Alg/B NPs solution, respectively.

## Morphological Degradation Time (MDT) of Nanoparticles

The morphology of the Cs/Alg/B NPs is shown in Figure 1 and Supplementary Figure 5, indicating that different times were needed for degradation between runs. The morphological shape is an important factor for protection from encapsulant and having an appropriate controlled release. When appreciating how size, shape, and chemistry affect the delivery process, morphological changes can be used as an index and NPs can be redesigned for more effective delivery[39] (Table 1). Generally, the morphological stability of NPs influences the delivery process, and NPs which keep their structure during release are delivered effectively. Hence, morphological changes of NPs followed during release time and their changes till the final stage of morphological degradation were calculated as morphological degradation time (MDT) (Table 1). One of the effective factors in changing the shapes of NPs is the release profile. Generally, NPs which experience accelerated release have low morphological degradation time. The MDT varied in different formulation conditions (pH, Cs/Alg Mw ratios, and stirring rate).[49] The increasing Cs/Alg Mw ratios created Cs/Alg/B NPs with various thickness values. Meanwhile, aggregation of Cs/Alg/B NPs formulated with higher Cs/Alg Mw ratios (3/1) has accelerated morphological change (without appropriate controlled release) and has decreased the required time for degradation morphology of the Cs/Alg/B NPs (Supplementary Figure 4C and F). On the other hand, Cs/Alg/B NPs with a non-uniform wall thickness cannot absorb water adequately and cracks from different sides earlier. Increased pH also accelerates the MDT of Cs/Alg/B NPs due to increasing the size and decreasing the ζ-potential and PDI (Supplementary Figure 4A and D). It can be concluded that the stability and MDT of Cs/Alg/B NPs have been improved dramatically by increasing ζ-potential and decreasing the size and PDI. Increasing of stirring rate also decreases the MDT of Cs/Alg/B NPs by increasing the agglomeration (Supplementary Figure 4B and E). The relationships between variables for MDT based on acquired data is shown in equation 7:

$$Y6 = 4.20 - 5.25Y - 0.25Z - 0.25XY + 0.25XZ + 0.75YZ - 0.23X^2 + 3.77Y^2 - 0.22Z^2 \quad (7)$$

where Y6 is the MDT, X is the stirring rate, and Y and Z are Cs/Alg Mw ratios and pH of the final Cs/Alg/B NPs solution, respectively.

## Morphology of Optimized rhBMP-2-Loaded Chitosan/Alginate Nanoparticles (Cs/Alg/B NPs)

The size and morphological features of NPs are assumed to have an extremely important role in drug release and pharmacokinetics.[42] In this work, the prepared Cs/Alg/B NPs are analyzed by SEM in terms of size and morphology. The images indicate the proper and improper morphologies (Figure 4). In general, a spherical shape and uniform distribution is the desired morphology for NPs.[43] The Cs/Alg/B NPs were smooth and soft and had a normal distribution with an average size of 180–265 nm. In higher Cs/Alg Mw ratios, non-spherical particles were observed due to the appearance of free polymers in Cs/Alg/B NPs solution (Figure 1). The result was in a good agreement with other studies.[24,47,48]

## Cell Toxicity

Cytotoxicity of the Cs/Alg/B NPs is one of the important factors affecting their clinical applications. In the nanocarrier systems, ideal vehicles have a minimum size and toxicity and maximum LE.[44] Generally physical and chemical characteristics like size, shape, specific surface area, surface charge, catalytic activity, and the presence or absence of a shell and functional groups on the surface that affect the cellular toxicity of NPs.[48] In this research, the toxicity of alginate, chitosan, and optimized Cs/Alg/B NPs were evaluated by MTT assay. The results indicated

that the optimized Cs/Alg/B NPs had no significant toxicity on NIH 3T3 cells compared to the untreated cells for 24 hours. Chitosan alone was fairly toxic at 24 and 48 hours in comparison with alginate which had no significant toxicity on NIH 3T3 cells and the number of viable cells was higher compared to alginate and Cs/Alg/B NPs at 24 and 48 hours (Figure 5). The cell membrane as a functional barrier uses different mechanisms for the transportation of the materials into and out of the cell. One of the effective factors in cellular uptake kinetics is the surface charge of materials. Chitosan and alginate induce positive and negative surface charges around the cell membrane respectively that may change pharmacokinetics and cellular uptake.[11] Chitosan can enter the cell via endocytosis and can thus be found inside endosomes early after internalization but it is mostly free in the cytosol and only rarely co-localize with NPs. A positive polymeric agent like chitosan has a capacity which is named as a proton sponge effect and explains why certain cationic polymers can sequester the H+ ions whose increased concentration within the lumen of the endosome is responsible for the acidification taking place during the process of endo-lysosomal maturation. These changes can increase cellular toxicity.[48] Positively charged NPs in comparison with negatively charge NPs and neutral NPs due to electrostatic attraction between the negatively charged cell membrane glycoproteins and positively charged NPs can enter cells easily. The chitosan surface charge with $H^+$ ions released from acetic acid is higher than the density of surface charge produced by alginate around the cells. However, in Cs/Alg/B NPs, due to the involvement of functional groups of chitosan with rhBMP-2, the surface charge density was created by Cs/Alg/B NPs around the cell being less in comparison with chitosan and it cannot create the same toxicity for NIH 3T3 cells. Although, on the whole, it is widely accepted that alginate provides a matrix in which cells can survive. Many authors have reported similar observations.[31,45,46] The disintegration of alginate will remove the mechanical constraint of the matrix, enables the cell proliferation, and protects the cells from environmental changes. Generally, cross-linked gels such as alginate undergo dissolution at a rate that is influenced strongly by the ionic media; alginate gel forms when $Ca^{2+}$ ions interact with the glucuronic residues in adjacent alginate chains which is in agreement with other research.[30,31]

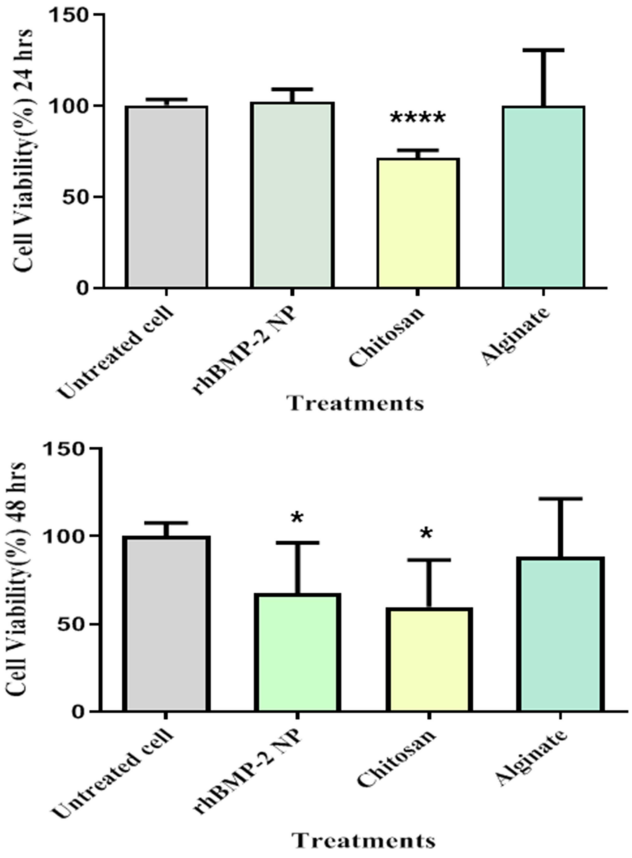


**Figure 5** Cytotoxicity effects of chitosan, alginate, and Cs/Alg/B NPs on NIH 3T3cells at 24 and 48 hours. The NIH 3T3 cells were cultured in 96-well plates and were exposed to 10 µg chitosan, alginate, Cs/Alg/B NPs (26 µg/mL), and negative control (RPMI 1640). Positive control (untreated cell). Cell viability calculated as; viability (%) =Mean OD/Control OD×100%. All data are presented as the mean of three different measurements±SD, asterisks (*) represent means the significant difference from the control group by the Bonferroni posttest ($P<0.05$) and asterisks (****) $P<0.0001$. OD, optical density; SD, standard deviation.; Cs/Alg/B NPs(rhBMP-2 NPs), rhBMP-2-loaded chitosan/alginate nanoparticles.

## Conclusion

In conclusion, the results of this study showed the best statistical optimization for rhBMP-2 delivery according to the variables; pH values, Cs/Alg Mw ratios, and stirring rates. The best formulation was optimized for Cs/Alg NPs and it can also be generalized to other BMPs family.

## Abbreviations

CR, cumulative release; Cs/Alg, chitosan/alginate; Cs/Alg/B NPs, rhBMP-2-loaded chitosan/alginate nanoparticles; DD, Degree of deacetylation; DMSO, Dimethyl sulfoxide; FDA, Food and Drug Administration; 3D, Three Dimension; LE, Loading efficacy; MTT, 3-(4, 5-dimethylthiazol-2-yl)-2, 5-diphenyltetrazolium bromide; NP, Nanoparticle; PDI, Polydispersity index; rhBMP2, recombinant human bone protein-2; SEM, Scan electron microscope; GI, Ionotropic gelation; GM, Gelatin microsphere; MWCO, Molecular weight cut-off.

## Funding

This work was supported by the deputy of research, Tehran University of Medical Sciences grant number 30320.

## Disclosure

The authors declare no conflicts of interest in this work.

## References

1. Wang Z, Wang Z, Lu WW, et al. Novel biomaterial strategies for controlled growth factor delivery for biomedical applications. *NPG Asian Mater*. 2017;9:1–17. doi:10.1038/am.2017.171
2. Huntley R, Jensen E, Gopalakrishnan R, Mansky KC. Bone morphogenetic proteins: their role in regulating osteoclast differentiation. *Bone Rep*. 2019;10(100207):1–9. doi:10.1016/j.bonr.2019.100207
3. Chang HM, Cheng JC, Taylor E, Leung PCK. Oocyte-derived BMP15 but not GDF9 down-regulates connexin43 expression and decreases gap junction intercellular communication activity in immortalized human granulosa cells. *Mol Hum Reprod*. 2014;20 (5):373–383. doi:10.1093/molehr/gau001
4. Venkatesan J, Anil S, Kim SK, SukShim M. Chitosan as a vehicle for growth factor delivery: various preparations and their applications in bone tissue regeneration. *Int J Biol Macromol*. 2017;104(Part B):1383–1397. doi:10.1016/j.ijbiomac.2017.01.072
5. Fung SL, Wu X, Maceren JP, Mao Y, Kohn J. In vitro evaluation of recombinant bone morphogenetic protein-2 bioactivity for regenerative medicine. *Tissue Eng Part C Methods*. 2019;25(9):553–559. doi:10.1089/ten.TEC.0156
6. Sur S, Rathore A, Dave V, Reddy KR, Chouhan RS, Sadhu V. Recent developments in functionalized polymer nanoparticles for efficient drug delivery system. *Nano-Struct Nano-Objects*. 2019;20:1–19. doi:10.1016/j.nanoso.2019.100397
7. Erdoğar N, Akkın S, Bilensoy E. Nanocapsules for drug delivery: an updated review of the last decade. *Recent Pat Drug Deliv Formul*. 2018;12(4):252–266. doi:10.2174/1872211313666190123153711
8. Zazo H, Colino CI, Lanao JM. Current applications of nanoparticles in infectious diseases. *J Control Release*. 2016;224:86–102. doi:10.1016/j.jconrel.2016.01.008
9. Kunjachan S, Jose S, Lammers T. Understanding the mechanism of ionic gelation for synthesis of chitosan nanoparticles using qualitative techniques. *Asian J Pharm*. 2010;4(2):148–153.doi:10.4103/0973-8398.68467
10. Rafiee A, Alimohammadian MH, Gazori T, et al. Comparison of chitosan, alginate and chitosan/alginate nanoparticles with respect to their size, stability, toxicity and transfection. *Asian Pac J Trop*. 2014;4(5):372–377. doi:10.1016/S2222-1808(14)60590-9
11. Krebs MD, Salter E, Chen E, Sutter KA, Alsberg E. Calcium phosphate-DNA nanoparticle gene delivery from alginate hydrogels induces in vivo osteogenesis. *J Biomed Mater Res A*. 2010;1:92 (3):1131–1138. doi:10.1002/jbm.a.32441
12. Su Sh, Kang PM. Systemic review of biodegradable nanomaterials in nanomedicine. *Nanomaterials*. 2020;10(656):1–21. doi:10.3390/nano10040656
13. Giri TK, Kumar K, Alexander A, Ajaz A, Badwaik H, Tripathy M, Tripathi DK. Novel controlled release solid dispersion for the delivery of diclofenac sodium. *Curr Drug Deliv*. 2013b;10(4):435–443. doi:10.2174/1567201811310040008
14. Sarmento B, Ribeiro AJ, Veiga F, Ferreira DC, Neufeld RJ. Insulin-loaded nanoparticles are prepared by alginate ionotropic pregelation followed by chitosan polyelectrolyte complexation. *J Nanosci Nanotechnol*. 2007;7(8):2833–2841. doi:10.1166/jnn.2007.609
15. Lai RF, Li ZJ, Zhou ZY, Feng ZQ, Zhao QT. Effect of rhBMP-2 sustained-release nanocapsules on the ectopic osteogenesis process in Sprague-Dawley rats. *Asian Pac J Trop*. 2013;6(11):884–888. doi:10.1016/S1995-7645(13)60157-1
16. Song WY, Liu GM, Li J, Luo YG. Bone morphogenetic protein-2 sustained delivery by hydrogels with microspheres repairs rabbit mandibular defects. *Tissue Eng Regen Med*. 2016;13(6):750–761. doi:10.1007/s13770-016-9123-0
17. Khuri AI, Cornell JA. *Responses Surfaces: Design and Analyses*. 2nd ed. Monticello, NY: Marcel Dekker; 1996.
18. Myers RH, Montgomery D, Vining GG, Borror CM, Kowalski SM. Response surface methodology: a retrospective and literature survey. *J Qual Technol*. 2004;36(1):53–78. doi:10.1080/00224065.2004.11980252
19. Ryan TP. *Modern Experimental Design*. New York: John Wiley & Sons; 2007.
20. Li X, Min Sh, Zhao X, Lu Zh, Jin A. Optimization of entrapping conditions to improve the release of BMP-2 from PELA carriers by response surface methodology. *Biomed Mater*. 2015;10(1):015002. doi:10.1088/1748-6041/10/1/015002
21. Poth N, Seiffart V, Gross G, Menzel H, Dempwolf W. Biodegradable chitosan nanoparticle coatings on titanium for the delivery of BMP-2. *Biomolecules*. 2015;5(1):3–19. doi:10.3390/biom5010003
22. Xia YJ, Xia H, Chen L, et al. Efficient delivery of recombinant human bone morphogenetic protein (rhBMP-2) with dextran sulfate-chitosan microspheres. *Exp Ther Med*. 2018;15(4):3265–3272. doi:10.3892/etm.2018.5849
23. Zhou PY, Wu JH, Xia Y, et al. Loading BMP-2 on nanostructured hydroxyapatite microspheres for rapid bone regeneration. *Int J Nanomedicine*. 2018;13:4083–4092. doi:10.2147/IJN.S158280
24. Zohri M, Nomani AR, Gazori R, et al. Characterization of chitosan/alginate self-assembled nanoparticles as a protein carrier. *J Disper Sci Technol*. 2011;32:576–582. doi:10.1080/01932691003757314
25. Suliman S, Xing Zh, Wu X, et al. Release and bioactivity of bone morphogenetic protein-2 are affected by 2 scaffold binding techniques in vitro and in vivo. *J Control Release*. 2015;197:148–157. doi:10.1016/j.jconrel.2014.11.003
26. Jiang LQ, Wang TY, Webster TJ, et al. Intracellular disposition of chitosan nanoparticles in macrophages: intracellular uptake, exocytosis, and intercellular transport. *Int J Nanomedicine*. 2017;12:6383–6398. doi:10.2147/IJN.S142060
27. Ibrahim HM, El-Bisi MK, Taha Gh, El-Alfy E. Chitosan nanoparticles loaded antibiotics as drug delivery biomaterial. *J Appl Pharm Sci*. 2015;5(10):085–090. doi:10.7324/JAPS.2015.501015
28. Divya K, Jisha MS. Chitosan nanoparticles preparation and applications. *Environ Chem Lett*. 2018;16:101–112. doi:10.1007/s10311-017-0670-y
29. Al-Rashed MM, Niknezhad S, Jana SC. Mechanism and factors influencing formation and stability of chitosan/lignosulfonate nanoparticles. *Macromol Chem Phys*. 2018;220:1800338.1–8. doi:10.1002/macp.201800338
30. Gazori T, Khoshayand MR, Azizi E, et al. Evaluation of alginate/chitosan nanoparticles as antisense delivery vector: formulation, optimization and in vitro characterization. *Carbohydr Polym*. 2009;77 (3):599–606. doi:10.1016/j.carbpol.2009.02.019
31. Rahmawati R, Permana MG, Harison B, et al D. Optimization of frequency and stirring rate for synthesis of magnetite ($Fe_3O_4$) nanoparticles by using coprecipitation- ultrasonic irradiation methods. *Procedia Eng*. 2017;170:55–59. doi:10.1016/j.proeng.2017.03.010
32. El Bialy l, Jiskoot W, Reza Nejadnik M. Formulation, delivery and stability of bone morphogenetic proteins for effective bone regeneration. *Pharm Res*. 2017;34(6):1152–1170. doi:10.1007/s11095-017-2147-x
33. Chen MC, Mi FL, Liao ZX, et al. Recent advances in chitosan-based nanoparticles for oral delivery of macromolecules. *Adv Drug Deliv Rev*. 2013;65(6):865–879. doi:10.1016/j.addr.2012.10.010

34. Kamaly N, Yameen B, Wu J, Farokhzad OC. Degradable controlled-release polymers and polymeric nanoparticles: mechanisms of controlling drug release. *Chem Rev*. 2016;116(4):2602–2663. doi:10.1021/acs.chemrev.5b00346
35. Caetano LA, Almeida AJ, Gonçalves LMD. Effect of experimental parameters on alginate/chitosan microparticles for BCG encapsulation. *Mar Drugs*. 2016;14(5):90. doi:10.3390/md14050090
36. Venkatesan J, Bhatnagar I, Kim SK. Chitosan-alginate bio composite containing fucoidan for bone tissue engineering Mar. *Drugs*. 2014;12(1):300-316. doi:10.3390/md12010300
37. Demir GM, Karaküçük A, Değim Z, et al. Stirring speed effects on physical characteristics of theophylline microsphere. Proceedings of the 5th International Conference on Nanotechnology: Fundamentals and Applications Prague, Czech Republic; 2014:11–13.
38. Jelvehgari M, Barar J, Nokhodchi A, Shadrou S, Valizadeh H. Effects of process variables on micrometric properties and drug release of non-degradable microparticles. *Adv Pharm Bull*. 2011;1(1):18–26. doi:10.5681/apb.2011.003
39. Fan W, Yan W, Xu Z, Ni H. Formation mechanism of monodisperse, low molecular weight chitosan nanoparticles by ionic gelation technique. *Colloids Surf B Biointerfaces*. 2012;90:21–27. doi:10.1016/j.colsurfb.2011.09.042
40. Albanese A, Peter S, Tang PS, Chan WCW. The effect of nanoparticle size, shape, and surface chemistry on biological systems. *Annu Rev Biomed Eng*. 2012;14:1–16. doi:10.1146/annurev-bioeng-071811-150124
41. Masarudin MJ, Cutts SM, Evison BJ, Phillips DR, Pigram PJ. Factors determining the stability, size distribution, and cellular accumulation of small, monodisperse chitosan nanoparticles as candidate vectors for anticancer drug delivery: application to the passive encapsulation of [14C]-doxorubicin. *Nanotechnol Sci Appl*. 2015;8:67–80. doi:10.2147/NSA.S91785
42. Khanmohammadi MR, Elmizadeh H, Ghasemi K. Investigation of size and morphology of chitosan nanoparticles used in drug delivery system employing chemometric technique. *Iran J Pharm Res*. 2015;14(3):665–675. doi:10.22037/IJPR.2015.1761
43. Kean T, Thanou M. Biodegradation, biodistribution and toxicity of chitosan. *Adv Drug Deliv Rev*. 2010;62(1):3–11. doi:10.1016/j.addr.2009.09.004
44. Bohari SPM, Hukins DWL, Grover LM. Effect of calcium alginate concentration on viability and proliferation of encapsulated fibroblasts. *Biomed Mater Eng*. 2011;21(3):159–170. doi:10.3233/BME-2011-0665
45. Fröhlich E. The role of surface charge in cellular uptake and cytotoxicity of medical nanoparticles. *Int J Nanomedicine*. 2012;7:5577-5591 doi:10.2147/IJN.S36111
46. Imam SS, Aqil M, Akhtar M, Sultana Y, Ali A. Formulation by design-based proniosome for accentuated transdermal delivery of risperidone; in vitro characterization and in vivo pharmacokinetic study. *Drug Deliv*. 2015;22(8):1059–1070. doi:10.3109/10717544.2013.870260
47. Sukhanova A, Bozrova S, Sokolov P, Berestovoy M, Karaulov A, Nabiev I. Dependence of nanoparticle toxicity on their physical and chemical properties. *Nanoscale Res Lett*. 2018;13(44):1–21. doi:10.1186/s11671-018-2457-x
48. Malatesta M, Grecchi S, Chiesa E, Cisterna B, Costanzo M, Zancanaro C. Internalized chitosan nanoparticles persist for long time in cultured cells. *Eur J Histochem*. 2015;59(1):2492, 61–65. doi:10.4081/ejh.2015.2492
49. Duncan TV. Release of engineered nanomaterials from polymer nanocomposites: the effect of matrix degradation. *ACS Appl Mater Interfaces*. 2015;7(1):20–39. doi:10.1021/am5062757